

Study on Cooling of Positronium for Bose-Einstein Condensation

K. Shu^{1,*}, X. Fan^{1,*}, T. Yamazaki², T. Namba², S. Asai¹,
K. Yoshioka¹, M. Kuwata-Gonokami¹

¹Department of Physics, Graduate School of Science, The University of Tokyo, 7-3-1 Hongo, Bunkyo-ku, Tokyo 113-0033, Japan

²International Center for Elementary Particle Physics (ICEPP), The University of Tokyo, 7-3-1 Hongo, Bunkyo-ku, Tokyo 113-0033, Japan

*Corresponding authors

E-mail: kshu@icepp.s.u-tokyo.ac.jp(K. Shu), xfan@icepp.s.u-tokyo.ac.jp(X. Fan)

Abstract. A new method of cooling positronium down is proposed to realize Bose-Einstein condensation of positronium. We perform detail studies about three processes (1) thermalization processes between positronium and silica walls of a cavity, (2) Ps-Ps scatterings and (3) Laser cooling. The thermalization process is shown to be not sufficient for BEC. Also Ps-Ps collision is shown to make a big effect on the cooling performance. We combine both methods and establish an efficient cooling for BEC. We also propose a new optical laser system for the cooling.

PACS numbers: 36.10.Dr, 67.85.Jk

Keywords: positronium, Bose-Einstein condensation, laser cooling

1. Introduction

Positronium (Ps), a bound state of an electron and a positron, is the lightest atom, whose mass $m_{\text{Ps}} = 1022 \text{ keV}$. The two ground states of Ps, the triplet state (1^3S_1) and the singlet state (1^1S_0), are known as *ortho*-positronium (*o*-Ps) and *para*-positronium (*p*-Ps) respectively. *Ortho*-positronium decays slowly into three photons with a lifetime of 142 ns[1]. On the other hand, *p*-Ps quickly decays into two photons. Two states can be mixed with a weak magnetic field. Ps is therefor a good source of 511 keV γ ray. Furthermore Ps is a good tool to probe the gravity for anti-particle, since Ps is a purely particle and anti-particle system.

Bose-Einstein condensation (BEC) is one of the most interesting phenomena of the quantum physics and macroscopic behavior of small particles can be directly observed in BEC state. We can enhance small effects of the particle level up to the observable level and BEC provides various applications. First observation of BEC of weakly interacting bosonic atomic gas was found using ^{87}Rb gas in 1995[2] and has opened a new era of studying the macroscopic behavior of quantum gas. Ps BEC is very attractive since it would provide the 511 keV γ ray laser[3, 4] and macroscopic behavior of anti-particle gravity can be observed.

The de Broglie wave length, λ_D , and the density, n , play a important role for BEC and the

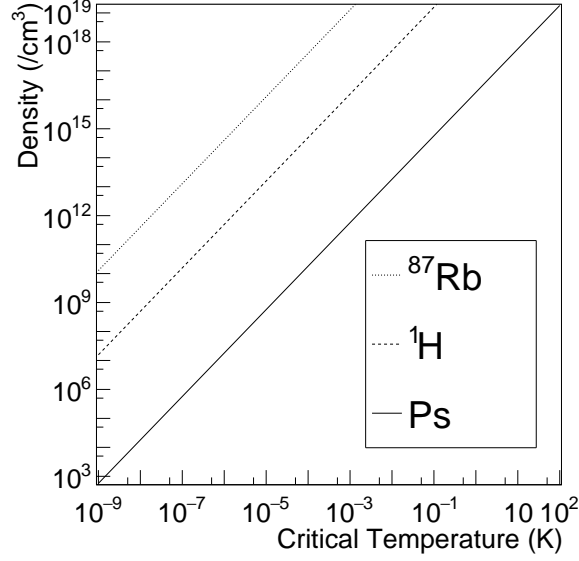


Figure 1. Relation between density and critical temperature of BEC transition. Left side of each line is a region where the atoms are in BEC phase.

critical temperature, T_C , is determined by the following formula:

$$n\lambda_D^3 = n \left(\frac{2\pi\hbar^2}{mk_B T_C} \right)^{3/2} > 2.612, \quad (1)$$

\hbar : Planck constant, m : a mass of an atom, k_B : Boltzmann constant.

Figure 1 shows T_C as a function of n , for ^{87}Rb , ^1H and Ps. Since Ps is very light, BEC can be achieved at a few Kelvin for $n \sim 10^{15} / \text{cm}^3$. This T_C is much higher than that for ^{87}Rb and ^1H .

It is essential to rapidly cool Ps atoms down to the order of a Kelvin. There were some studies about cooling of Ps. A cold Si cavity was used for trapping and cooling down Ps by the collision between the walls and Ps[5], but we will later show the cooling with the cold cavity is insufficient. A cooling with laser was also proposed [6, 7], in which a large free space was assumed. High density of Ps is also crucial and the scatterings between Ps and Ps should be also taken into account. In this article, we propose a new cooling method using both and estimate the cooling performance to realize Ps BEC.

2. Setup

The conceptional view of our experimental setup is shown in Fig. 2. Positrons are stored in a small cavity made by silica. The positron beam in which about 10^7 positrons ($E=5 \text{ keV}$) are stored for each bunch will be used. This number of positrons is already possible in elsewhere[8]. The positrons are focused and injected into the trapping cavity made by silica which is cooled at 1 K. The cavity has an internal void whose dimension is assumed to be a rectangular shape of $100 \text{ nm} \times 100 \text{ nm} \times 100 \text{ nm}$. About 4×10^3 of spin-polarized Ps atoms are assumed to be created inside the void while the focusing technique and overall efficiency of the conversion from the positrons to Ps have to be studied in future. Ps atoms have an initial kinetic energy of around 0.8 eV[9] and are confined inside the cavity. The cavity is irradiated by UV laser beams which

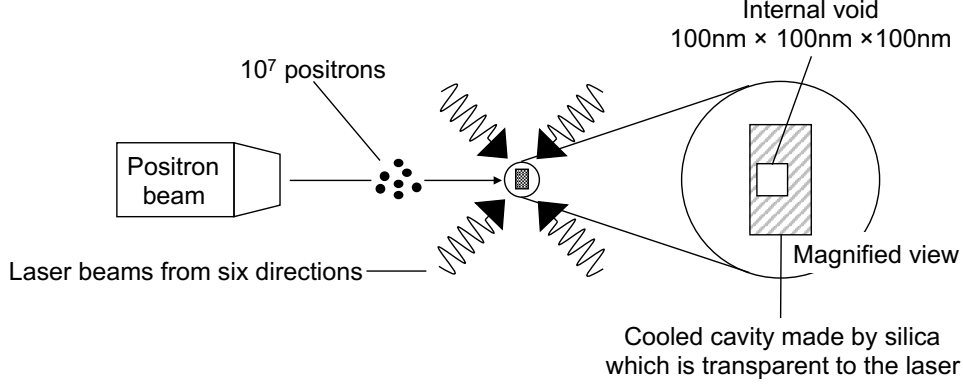


Figure 2. The schematic diagram of the experimental setup. The two laser beams which are perpendicular to the sheet are not written.

are configured as optical molasses: by three orthogonal pairs of counter-propagating beams. The laser photons can go through into the cavity because silica is transparent to this light. The laser system is described in section 4.2.

In this setup, Ps atoms have the following interactions:

- Thermalization by interactions with silica walls of the cold cavity,
- Ps-Ps two-body interactions,
- Cooling by optical transitions and momentum recoils by photons.

As discussed in the following sections, the cooling through the thermalization process is efficient for Ps atoms with high energy while the opposite for laser cooling. These two cooling processes are complementary, so we propose a new cooling scheme in two stages: initially by Ps-silica interactions and then by laser fields after the former becomes inefficient. We evaluate cooling efficiency of each process and see whether it is enough to achieve BEC transition.

3. Thermalization in the silica cavity

The thermalization process is evaluated by using the classical interaction model[9]. This model assumes thermalization will proceed through classical elastic collisions between Ps and grains of a surrounding material. According to the model, an average kinetic energy of Ps, E , evolves as follows:

$$\frac{dE}{dt} = -\frac{2}{LM} \sqrt{2m_{\text{Ps}}E} \left(E - \frac{3}{2}k_B T \right). \quad (2)$$

Here M is an effective mass of surrounding grains, L is the mean free path of the collisions with grains and T is temperature of a surrounding material. This model can well describe the thermalization process which were measured by various techniques[10–12].

Experimental results are used in order to determine M . Various results of the measurements[9, 10, 12, 13] are shown in Fig. 3. M is shown as a function of Ps kinetic energy in which it was measured, because the effective mass could be dependent to kinetic energy of interacting Ps as suggested[13]. This is because the number of phonon modes which Ps can excite at collisions decreases as kinetic energy of Ps does. We estimate energy dependence of M in a.m.u as $M = 21 + 308 \exp\left(-\frac{E}{0.16\text{eV}}\right)$ in order to reproduce the experimental result as shown in Fig. 3 by the solid line which is named as the best fit. The uncertainty is large because precision of the measurements is still limited. A range of the predictions is also shown in Fig.3 as fast and slow.

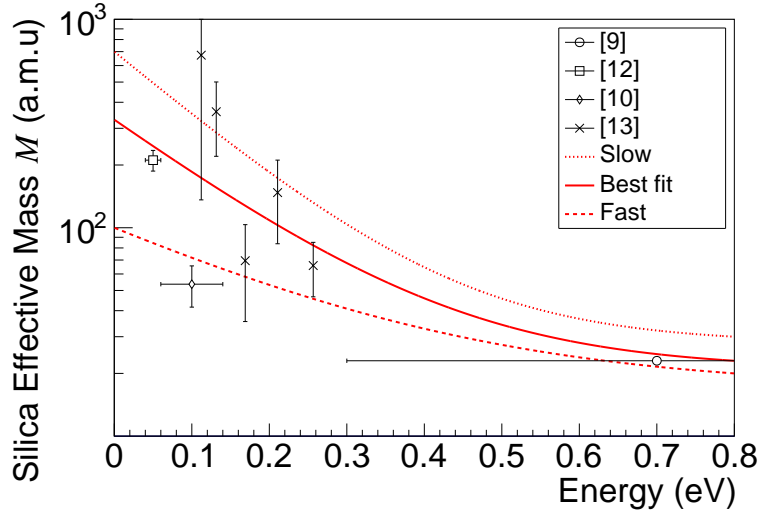


Figure 3. Effective mass of a silica grain versus kinetic energy of Ps. Error bars for the vertical axis are measurement errors and ones for the horizontal axis are measured energy regions if there are. Lines are estimated predictions of the energy dependence of M . Legends show the references of the experiments.

In addition to the interaction with the silica walls, Ps-Ps interactions must be taken into account in the case of high density. A main process is the elastic s -wave scattering for spin-polarized Ps atoms. This process leads to quasi thermal equilibrium among Ps atoms: the energy distribution of atoms becomes Maxwell-Boltzmann distribution with an approximation of classical scattering. The total cross section (σ) of the scattering is given by $\sigma = 4\pi a^2$ where a is a scattering length, $a = 0.16$ nm [14, 15]. The mean free time (τ) of scatterings depends on a number density of Ps, n , an average velocity, \bar{v} , and σ as $\tau = 1/n\sigma\bar{v}$. This interval with $n = 10^{18}$ /cc is less than 100 ps even at 10 K. The quasi thermalization among Ps atoms is quite fast comparing to the thermalization process between Ps atoms and the silica walls.

The interactions with the silica wall and Ps-Ps elastic scatterings are simulated by the Monte Carlo method. Time evolutions of temperature are shown in Fig. 4. As for the best fit estimation of M , Ps can be cooled to 300 K in 100 ns from the initial energy of 0.8 eV. The further cooling is so slow that it takes 500 ns to reach 100 K even though the cavity is at 1 K. Our estimation is consistent with previous studies in which Ps would not thermalize at low temperatures [16–18].

However the thermalization process strongly depends on the effective mass of a silica grain as shown in Fig. 4. It is necessary to perform additional measurements with high precision in order to determine M .

There is another interaction model with silica [19, 20]. In this model, Ps atoms emit or absorb an acoustic phonon on the cavity wall through deformation potential scattering. Interaction rates can be deduced by the first-order perturbation theory. We also evaluate the thermalization process in this model with fitting to reproduce the experimental results [10–12]. There is no observable difference between the two models for Ps atoms of higher than around 300 K. In lower energy, the thermalization process in this phonon model is more insufficient than in the classical model because of less stimulated emission at low temperatures in the phonon model. In our cooling scheme, the thermalization process is crucial only in the initial stage of cooling to around 300 K. The difference to the final result is therefore negligible.

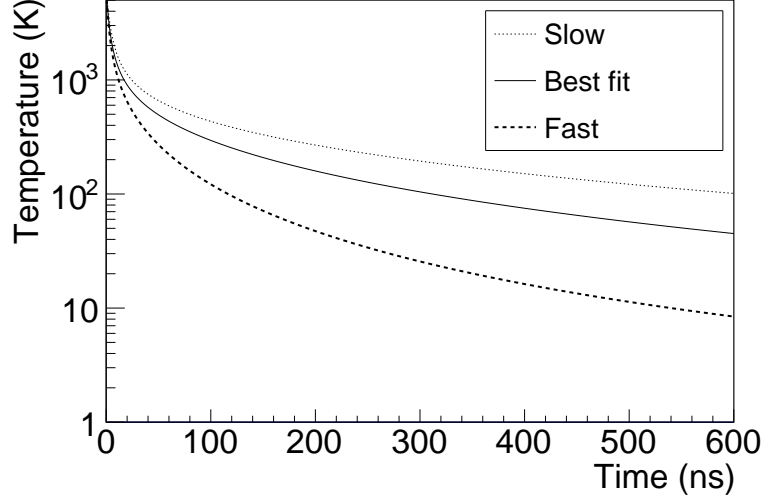


Figure 4. Time evolutions of temperature in the silica cavity. The evaluations are performed with different three estimations of M . Legends show which estimation curve is used. Slow, best fit and fast correspond to the curves in Fig. 3.

4. Laser Cooling

4.1. The evaluation of laser cooling

It is necessary to accelerate the cooling down from a few hundreds of Kelvins. It is efficient to use $1s \leftrightarrow 2p$ transition for laser cooling of Ps because of a large recoil momentum by photons. The difference between these two energy levels corresponds to 243 nm UV light.

Optical transitions induced by the laser can be modeled with the rate equation approach[21] because the time scale of cooling down, more than 100 ns, is much longer than the time constant 3.2 ns of the spontaneous decay from $2p$ to $1s$. The stimulated transition rate, which is called as “Einstein B coefficient”, can be calculated by the flux of photons and the cross section of the interaction between Ps and resonant photons. This coefficient can be calculated as follows:

$$B(t, \vec{x}, \vec{v}) = \int d\omega \frac{I(t, \vec{x}, \omega)}{\hbar\omega} \cdot \frac{4}{3}\pi^2 \alpha \omega_0 |X_{12}|^2 \cdot \frac{1}{2\pi} \frac{\Gamma/2}{(\omega(1 - \vec{k} \cdot \vec{v}/c) - \omega_0)^2 + (\Gamma/2)^2}, \quad (3)$$

t : time, \vec{x} : a position of Ps, \vec{v} : a velocity of Ps, \vec{k} : a direction of laser photons.

$I(t, \vec{x}, \omega)$ is an intensity per frequency of the laser, X_{12} and ω_0 mean the matrix element and resonant frequency of this transition for each. Gaussian profiles are assumed for frequency/timing/space domains of the intensity. $\Gamma = 313$ MHz is the natural line width so the last term in the equation (3) represents Breit-Wigner line shape including Doppler effect. The internal state evolves according to this stimulated transition rate and the spontaneous decay rate from $2p$ state. A Ps is recoiled by $\hbar\omega_{\text{Laser}}/m_{\text{Ps}}c = 1.5 \times 10^3$ m/s when it emits or absorbs a photon. The direction of a recoil is random for spontaneous emission while for stimulated absorption/emission same as photons in the laser. An important feature is that a self decay to gamma rays from $2p$ state is very slow compared to that from $1s$ state. This means that the maximum excitation effectively increases the lifetime of Ps twice to 284 ns.

Table 1 shows a summary of laser parameters. The laser is a pulse laser and its energy is $40 \mu\text{J}$, which is divided into the six beams and focused into $200 \mu\text{m}$ at the cavity. The timing of the peak intensity is delayed by 200 ns from the creation of Ps atoms as shown in the upper

Table 1. The summary of laser parameters of the 243 nm laser system.

Parameter Name	Value
Pulse energy	40 μJ
Center frequency	1.23 PHz $-\Delta(t)$
Frequency detune $\Delta(t)$	$\Delta(0 \text{ ns})=300 \text{ GHz}$ $\Delta(300 \text{ ns})=240 \text{ GHz}$
Bandwidth (2σ)	140 GHz
Time duration (2σ)	300 ns
Beam size (2σ)	200 μm

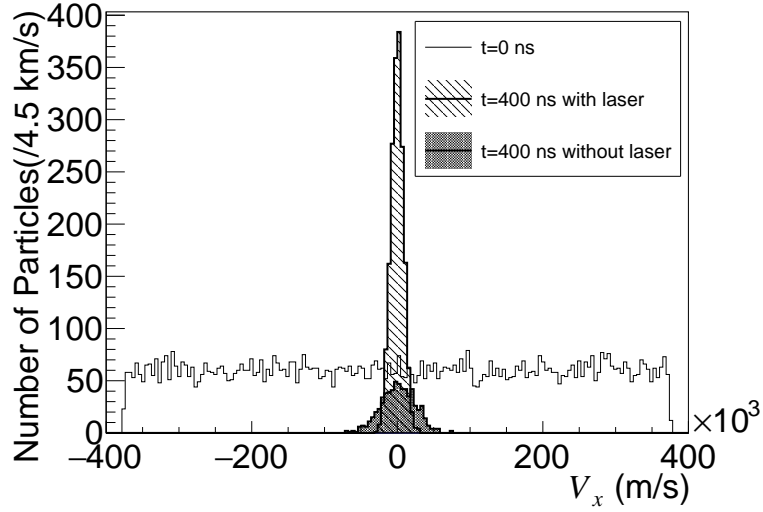


Figure 5. Distributions of Ps velocity with and without laser cooling. The horizontal axis represents x -component of Ps velocity. The number of remained atoms with laser is larger than that without laser because of the extended lifetime of self decay by excitations to $2p$ state.

part of Fig. 6. The time duration is 300 ns in order to cover a long duration necessary for cooling. The center frequency of the laser field is detuned from 1.23 PHz which corresponds to 243 nm wavelength. This detune, $\Delta(t)$, is 300 GHz at the beginning and then up-chirped to 240 GHz in order to compensate the decrease of Ps velocities. The bandwidth around the center frequency is 140 GHz in order to excite Ps atoms with a wide range of velocities. The required frequency chirp and bandwidth are quite large compared to standard systems for cooling other atoms. They come from the large Doppler shift of Ps due to its light mass compared to any other atoms. The laser system with these features is a new trial.

The cooling effect by the laser is evaluated by the Monte Carlo simulation. The best fit estimation of M in Fig. 3 is used for the thermalization process. Distributions of Ps velocity at different times are shown in Fig. 5. The distributions quickly become Maxwell-Boltzmann distributions by Ps-Ps scatterings. This means that Ps atoms are always in quasi thermal equilibrium and have well-defined temperature. After 400 ns, The width corresponds to that of 10 K(70 K) with(without) the laser. The number of remained atoms is increased with the laser because of the longer lifetime as described before. The time evolution of temperature and T_C are shown in Fig. 6. T_C is calculated from the density of Ps in $1s$ state. The cooling effect by the laser becomes dominant from around several hundreds of Kelvins. After around 400 ns, the temperature becomes less than T_C . This means that the phase transition to BEC can be achieved by our cooling scheme. Figure 7 shows condensate fractions which are calculated with

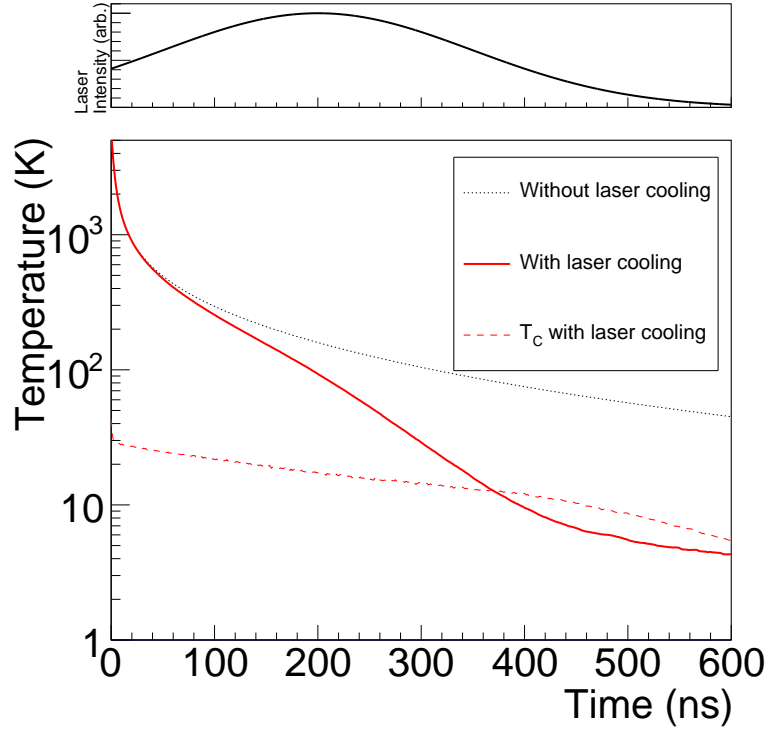


Figure 6. The upper part: Irradiated laser intensity in an arbitrary unit versus time. The lower part: Time evolutions of temperature and T_C . T_C decreases as the density of $1s$ Ps does due to the annihilation.

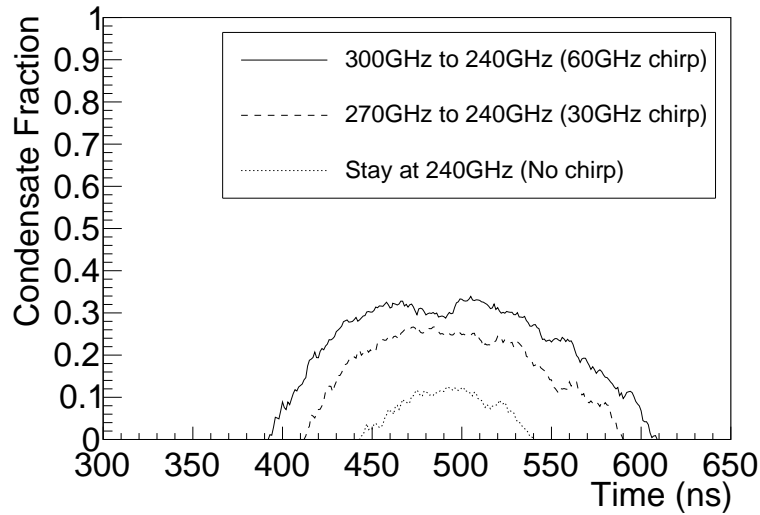


Figure 7. Condensate fractions with different frequency chirps. $\Delta(300\text{ ns})$ is fixed at 240 GHz and chirp ranges are 60 GHz, 30 GHz and 0 GHz.

an assumption of Ps atoms as non-interacting bosonic systems. More than 30% of the remained atoms will be in the condensate with the laser system described above.

The range of chirp is changed in order to see the effects. $\Delta(0\text{ ns})$ s are changed to 270 GHz and 240 GHz while $\Delta(300\text{ ns})$ s are fixed at 240 GHz. The results are also shown in Fig. 7. The

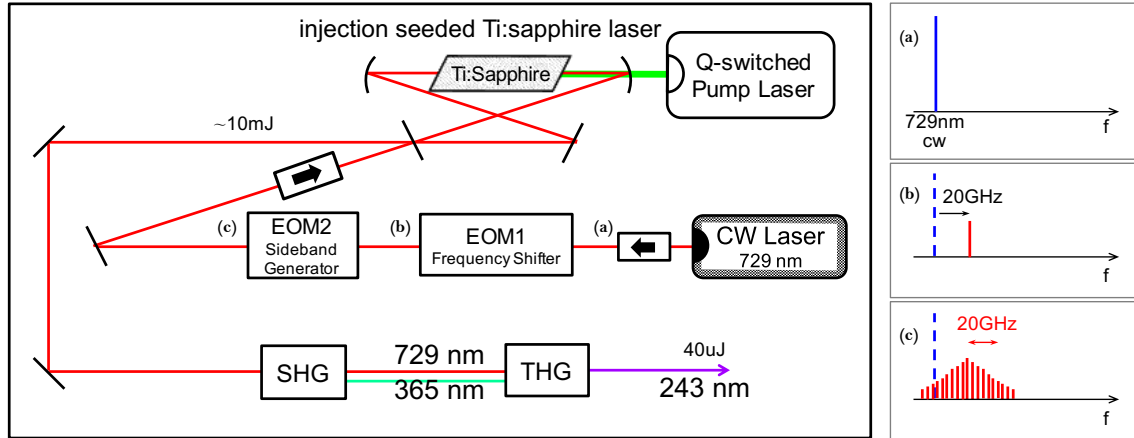


Figure 8. The schematic diagram of the laser system. 729 nm single mode CW light is frequency controlled at EOMs. Pulse shaping and amplifying are conducted at the following injection seeded Ti:Sapphire laser. Ti:sapphire crystal is pumped by Q-switched 532 nm pulsed laser. The light is converted to 243 nm at the last SHG and THG part. The pictures on the right side show the frequency information of the 729 nm light: (a) before entering EOMs, (b) ejected from EOM1 which generate up-chirp to 20 GHz, (c) ejected from EOM2 which generate sidebands about 20 GHz range. The frequency shift and broadening is multiplied by three at the last THG and the desired parameters in Table 1 can be obtained.

effects are as large as the fraction without chirp decreases to around 0.1 and the time interval of condensation is shortened to less than 100 ns due to its slower cooling. Even 30 GHz chirp can increase the fraction by twice than that without chirp. Therefore 30-60 GHz chirp is ideal for the cooling.

4.2. Implementation of the laser system

Though the specific parameters listed in table 1 are technically challenging, it can be achievable using various techniques which already exist. The technically challenging points are the large and fast frequency shift with the optical amplification for the long time duration more than 100 ns. The basic idea is to use third harmonics generation of 729 nm light, whose frequency and pulse shape are precisely controlled. Figure 8 shows schematic diagram of our designed laser system. A single mode 729 nm CW laser is used as a master laser. The CW light is modulated at the electro-optic modulator, EOM, to generate 20 GHz sideband. This generated sideband is used as a center frequency of the frequency chirp. The advantage to use sideband as center frequency is that the chirp can be electrically controlled by changing modulation frequency applied to EOM 1. At EOM 2, 20 GHz broad sidebands are generated around the first sideband. 1 GHz modulation frequency to EOM with 20 sidebands generation is enough to cover all the Ps Doppler broadening. After the sideband generation, the seed light is injected into injection seeded Ti:sapphire laser. The gain of the laser can be controlled by adjusting a waveform of a pump laser and reflective indexes of an output coupler so the desired amplification along 300 ns can be obtained. The energy in a pulse is about 10 mJ. Now the amplified pulse is well controlled in both time domain and frequency domain, and enters the following Second Harmonics Generation, SHG and Third Harmonics Generation, THG, to achieve desired 243 nm light. The 10 mJ injected pulse energy is high enough to obtain 40 μJ energy. Furthermore, the 20GHz frequency shift and 20GHz broadening are also multiplied by three at THG, so the frequency parameters in Table 1 can be obtained. The 243 nm light will be sent to Ps generation cavity and used as cooling light.

The repetition rate of the positron beam will be less than 10 Hz, so the assumed pulse energy is not so hard to achieve. Coincidence between source and laser system will be also easy by synchronising positron system and pulsed pump laser and EOMs. The most challenging part will be the large and fast frequency modulation at the two parts of EOM. In order to achieve this large frequency modulation, broadband traveling-wave type optical modulator will be used as a frequency shifter. Though this type of modulators have been mainly used in optical communication wavelength, modulation up to 100 GHz also exists in 1064 nm[22]. We are developing this broadband device compatible with 729 nm.

5. The Roadmap for Ps BEC

There are three steps to achieve Ps BEC. At first, the cooling process with silica should be confirmed. We are now measuring the thermalization process precisely. The second step is developing the laser system. Some studies are under going with basic technology already developed. The last step is developing the focus system of the slow positron beam. The beam should be focused into 100 nm while it can currently be focused into around 30 μm [23] in the other beam line. This positron feeding system will be combined with the laser system.

The detection of the transition to BEC can also be possible by the same technique as the precise measurement of Ps temperature. Another method could be using a characteristic spectrum of decaying gamma rays from the condensate. It is also under studying.

Acknowledgements

We would like to express sincere gratitude Prof. Y. Nagashima and Prof. H. Saito for helpful discussions. We also wish to express our great appreciation to Dr. J. Omachi and Y. Morita for insightful discussions.

References

- [1] Kataoka Y, Asai S and Kobayashi T 2009 *Physics Letters B* **671** 219 – 223
- [2] Anderson M H, Ensher J R, Matthews M R, Wieman C E and Cornell E A 1995 *Science* **269** 198–201
- [3] Mills A P, Cassidy D B and Greaves R G 2004 *Materials Science Forum* **445-446** 424–429
- [4] Avetissian H K, Avetissian A K and Mkrtchian G F 2014 *Phys. Rev. Lett.* **113** 023904
- [5] Platzman P M and Mills A P 1994 *Phys. Rev. B* **49** 454–458
- [6] Liang E P and Dermer C D 1988 *Optics Communications* **65** 419–424
- [7] Kumita T, Hirose T, Irako M, Kadoya K, Matsumoto B, Wada K, Mondal N, Yabu H, Kobayashi K and Kajita M 2002 *Nuclear Instruments and Methods in Physics Research Section B: Beam Interactions with Materials and Atoms* **192** 171–175
- [8] Cassidy D B, Deng S H M, Greaves R G and Mills A P 2006 *Review of Scientific Instruments* **77**
- [9] Nagashima Y, Kakimoto M, Hyodo T, Fujiwara K, Ichimura A, Chang T, Deng J, Akahane T, Chiba T, Suzuki K, McKee B T A and Stewart A T 1995 *Phys. Rev. A* **52** 258–265
- [10] Chang T, Xu M and Zeng X 1987 *Physics Letters A* **126** 189–194
- [11] Takada S, Iwata T, Kawashima K, Saito H, Nagashima Y and Hyodo T 2000 *Radiation Physics and Chemistry* **58** 781–785
- [12] Shibuya K, Kawamura Y and Saito H 2013 *Phys. Rev. A* **88** 042517
- [13] Nagashima Y, Hyodo T, Fujiwara K and Ichimura A 1998 *Journal of Physics B: Atomic, Molecular and Optical Physics* **31** 329
- [14] Oda K, Miyakawa T, Yabu H and Suzuki T 2001 *Journal of the Physical Society of Japan* **70** 1549–1555
- [15] Ivanov I A, Mitroy J and Varga K 2002 *Phys. Rev. A* **65** 022704
- [16] Kiefl R and Harshman D 1983 *Physics Letters A* **98** 447–450
- [17] Saito H and Hyodo T 1999 *Phys. Rev. B* **60** 11070–11077
- [18] Saito H and Hyodo T 2001 *New Directions in Antimatter Chemistry and Physics* ed Surko C M and Gianturco F A (Kluwer Academic Publishers) pp 101–114
- [19] Mariazzi S, Salemi A and Brusa R S 2008 *Phys. Rev. B* **78** 085428
- [20] Morandi O, Hervieux P A and Manfredi G 2014 *Phys. Rev. A* **89** 033609
- [21] Iijima H, Hirose T, Irako M, Kajita M, Kumita T, Yabu H and Wada K 2001 *Journal of the Physical Society of Japan* **70** 3255–3260

- [22] Nees J, Williamson S and Mourou G 1989 *Applied Physics Letters* **54** 1962–1964
- [23] Oshima N, Suzuki R, Ohdaira T, Kinomura A, Narumi T, Uedono A and Fujinami M 2008 *Materials Science Forum* **607** 238–242